

# Local shape descriptors, a survey and evaluation

Paul Heider<sup>1</sup>, Alain Pierre-Pierre<sup>2</sup>, Ruosi Li<sup>1</sup>, and Cindy Grimm<sup>1</sup>

<sup>1</sup>Washington University in St. Louis, <sup>2</sup>Queens University

---

## Abstract

*Local shape descriptors can be used for a variety of tasks, from registration to comparison to shape analysis and retrieval. There have been a variety of local shape descriptors developed for these tasks, which have been evaluated in isolation or in pairs, but not against each other. We provide a survey of existing descriptors and a framework for comparing them. We perform a detailed evaluation of the descriptors using real data sets from a variety of sources. We first evaluate how stable these metrics are under changes in mesh resolution, noise, and smoothing. We then analyze the discriminatory ability of the descriptors for the task of shape matching. Our conclusion is that sampling the normal distribution and the mean curvature, using 25 samples, and reducing this data to 5-10 samples via Principal Components Analysis provides robustness to noise and the best shape discrimination results.*

Categories and Subject Descriptors (according to ACM CCS): I.3.5 [Computer Graphics]: Computational Geometry and Object Modeling —Curve, surface, solid, and object representations

---

## 1. Introduction

Local shape descriptors are used in 3D shape matching to both find unique points on the surface and then to match up these points on different models. They can also be used to speed up searches by reducing the model to a small number of features which are easily compared. Given the plethora of descriptors out there, what is a good choice? We evaluate that question in the shape feature matching context — given sets of “similar” points, how well does the descriptor do at clustering similar points while distinguishing between points in different sets?

We first survey existing local shape descriptors, grouping them by type (Section 2). Next, we provide a framework for comparing these descriptors to each other. In the process of doing this, we develop several new variations of existing descriptors (Section 3). In specific, we create a rotation-independed version of Point descriptors [CJ97] and their variants.

To evaluate the descriptors we perform two studies. The first study (Section 4) is a straightforward analysis of behavior under changing mesh quality, noise, and smoothing. The second study (Section 5) uses hand-picked similar feature points to determine which descriptors are both sensitive (can determine if features are the same) and specific (can distin-

guish one feature from another). We also provide a correlation analysis on the descriptors (Section 6).

Our conclusion is that sampling mean curvature or the normal distribution at roughly 25 samples per local neighborhood, followed by Principal Components Analysis to reduce the data to 7-10 numbers, are the two best descriptors in terms of robustness and discrimination power.

**Contributions:** 1) A survey of existing local descriptors. 2) A systematic evaluation of a variety of shape descriptors on different data sets. 3) Rotationally-invariant modification of Point signatures. 4) Normalized comparison functions that allow for direct comparison of all descriptors.

## 2. Local descriptors

A good local descriptor is one that is invariant to “unimportant” geometric changes, typically rotation and translation, sometimes scaling, and sometimes bending (such as posing an articulated character). It should take into account the local shape of the surface surrounding a given point. It should also be robust to noise and sampling errors: Geometric noise (vertices moving), Mesh topology noise (the mesh connectivity changes), and Global topology noise (the creation of handles and tunnels). Local descriptors should also have a

meaningful comparison function, one that scales roughly linearly with perceived shape change and is robust to noise.

To handle invariance, most descriptors measure geometric properties that are invariant to translation and rotation, such as curvature, length, volume, and angle. Scale invariance requires a relative measure — for example, the length of a curve over a radius — or scaling the object to a default size.

There are, broadly, two ways to determine a local neighborhood around a point. The first is to measure Euclidean distance, for instance, all of the surface contained within a sphere. The second is to measure Geodesic distance by walking out a set distance on the surface. Empirically, we have determined that for small-scale features the two are qualitatively similar. The difference only really matters when considering large-scale features such as entire limbs. At this scale pose-invariance (a bent limb should be the “same” as a straight one) can only be achieved by considering geodesic distances. We divide existing local descriptors into three classes. The first two only look at local data, the third at global data. The two local data classes split on whether they sample a metric locally or fit a model to the local neighborhood.

### 2.1. Ring-based descriptors (sample metric locally)

**Blowing bubbles** [MPS\*03] intersects the surface with a set of concentric spheres and extracts information about the surface in two steps. First, they simply count the number of closed contours, ignoring curves that are far away (1, 2, or more than 2). They further classify the contours using the length of the contours and a local concavity measure that determines if the curve centroid is above or below the point. Altogether, these measures can be used to classify the surface into eleven different groups. These descriptors (length of curve, centroid) are generalized to an integrative framework in [PWHY09].

**Geodesic fans** [GGGZ05] sample a metric (such as curvature) on the mesh using concentric geodesic rings instead of spheres. Geodesic fans re-sample the metric into evenly-spaced samples in the radial and angular direction. To compare two fans, every possible rotation is tried, and the one with the minimal error is kept. They also introduce a 1D “curve”, where the values around a ring are collapsed into a single number (average, minimum, and maximum values). This eliminates the need to try all possible rotations but does result in a loss of information. A modified version of this, which combined curvature along geodesics with normal variation, was recently used to do polyp detection [OS10].

**Splash descriptor** Stein and Medioni [SM92] sample the normal at regularly-spaced intervals. The normals are mapped to a spherical coordinate system using the normal  $n_0$  at the point and a tangent vector  $t$ , with  $t$  chosen by finding the point  $P_i$  which has the maximum value of

$\sqrt{\langle n_0, n_i \rangle^2 + \langle t, n_i \rangle^2}$ . They then map this 3D curve to 2D by computing the curvature and torsion along it. It is not clear how necessary (or useful) this last step is; it was primarily motivated by compatibility with the rest of their system.

**Point descriptor** Chua and Jarvis [CJ97] used a similar sampling, but recorded the distance from the contour to a plane fit to the contour and passing through the point. Yamany and Farag [YF99, YF02] proposed a modified version of this where they took a line through the point on the ring. They then stored the line length and angle with respect to the normal. They convert this to a 2D image by using the first angle and length as the axes, and the normal angle as the image’s intensity value. They used all points in the mesh for this descriptor; by weighting the points by their distance to the center point [BMP02, KPNK03] this descriptor can be localized.

### 2.2. Expanding descriptors (fit model to region)

**Fitting polynomials:** Cipriano et. al [CPJG09] grow their disks using geodesics. Each disk is then treated as a height field over the tangent plane. They fit a quadratic polynomial to the height field, weighting the points by their surface area and how close to the center they are. Because they project their points directly to the tangent plane they may get folding; this is mitigated by a post-processing step which detects these cases as outliers. Finally, they define two descriptors. The first is the curvature of the fitted quadratic. The second descriptor treats the height field as an intensity image, and measures the anisotropy of the image. This can be computed directly from the polynomial coefficients, but is somewhat less specific than the curvature measures.

**Mesh saliency:** Mesh saliency [LVJ05] uses the concept of center-surround from perception to measure how the center of a disk differs from a disk twice as big. Essentially, they sum up a metric (usually mean curvature) using a Gaussian weighted sum centered at the point. They then repeat this sum using a kernel twice the size. The value for the disk is then the ratio of the two sums, normalized.

**Volume and surface area:** Instead of measuring derivative information (eg, curvature) on the surface, an alternative is to measure integrative information, such as volume [Con86] or surface area [PWHY09]. These measures, being integrated, are nominally more stable in the presence of noise than derivative measures. To extract more information about the local patch it is possible to apply Principal Components Analysis [CGR\*04, CRT04]. Pottman et al [PWHY09] provide a nice summary and comparison of these integrative, invariant geometric measures.

### 2.3. Iterative operator descriptors (global)

**Smoothing:** As a mesh is smoothed, vertices change their positions. Vertices in high-curvature regions tend to move

more than in low-curvature ones. Essentially, record the distance moved by each vertex for each smoothing iteration, for some number of iterations. This descriptor is used by Li and Guskov [LG05] to find interesting points and by the brain mapping community [FSD99] to identify sulcal folds on cortical surfaces.

**Geodesics and diffusion:** The techniques in this class do not directly measure the geodesics, but instead measure a diffusion process flowing along the geodesics. The Laplace-Beltrami operator [Rus07] is used to compute the diffusion because it essentially records the mesh connectivity.

Bronstein et. al [BBK\*10] use diffusion geometry (how long does it take, on average, to walk from one point to another on the surface using a random walk?) to compare two surfaces. To turn this into a local descriptor, measure the average probability of walking from the point  $P$  to all the neighboring points at time  $t$ , for increasing values of  $t$  [dGGV08]. An alternative is to measure the average distance to all of the points in the neighborhood [GSCO07]. Sun et. al [SOG09] perform a heat diffusion operation on the surface, and track the accumulated heat at the point over time.

Comparing two diffusion signatures requires some care because the values change rapidly for small time values, then smooth out. For this reason, Sun et. al [SOG09] sample time using a logarithmic scale and normalize by dividing by the area under the curve.

### 3. Shape descriptors

There are a variety of methods for calculating shape descriptors; we have attempted to unify them into a consistent framework so that they can be usefully evaluated against each other. We consider both the definition of the descriptor and the comparison function. To normalize the latter we incorporate a step that converts the raw descriptor to the range  $[0, 1]$ , accounting for non-linearities as best as possible. Several descriptors have inherent in them either picking a canonical tangent direction [CJ97, YF02] or comparing all possible rotations [ZG04]. We get around this by sampling the ring data into a histogram.

We define a local shape descriptor as a mapping from a small subset of the surface centered at a point  $P$  to a vector  $d$  of numbers. These vectors can then be compared to determine how similar two points are, or used in a classifier. By varying the amount of surface used, the descriptors can pick out smaller or larger features. *Metric* here refers to a value, such as curvature, calculated at every point on the surface. The general algorithm for computing a descriptor is as follows:

**1a, Ring and expanding descriptors:** For each point  $P$ , sample the metric at  $R$  concentric rings or patches spaced a distance  $r$  apart. This produces a vector of dimension  $RS$ , where  $S$  is the number of samples per ring.

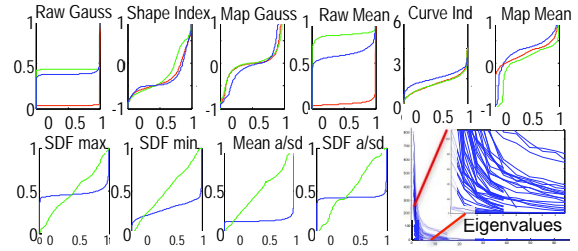


**Figure 1:** Top row: Sorted curvature values (raw, index, mapped). Red - Mandible, Blue - Tibia, Green = Ferret. Bottom row: Applying mapping (Section 3.2). Blue curve is original data, linearly scaled to the range  $[0,1]$ . Bottom right: Eigen values of all descriptors.

**1b, Iterative operator descriptors:** Apply the iterative operator. Record the values at  $R$  iterations, where each iteration corresponds (approximately) to the operator expanding a distance  $r$ . This produces a vector of dimension  $RS$  for each point  $P$ , where  $S$  is the dimension of the output of the operator at point  $P$  (usually  $S = 1$ ).

**2, Reduction:** Apply Principle Component Analysis (PCA) or Multi-dimensional Scaling (MDS) as appropriate to all of the vectors, and re-project the vectors onto this coordinate system.

**3, Normalize:** Normalize the distribution of values in each dimension, using a non-linear mapping as necessary, so they lie between zero and one and are (relatively) evenly distributed.

Section 3.1 defines the specific descriptors used in our study. Section 3.2 discusses the coordinate system change and normalization step.

**Sampling the surface:** We experimented with three different methods for sampling the surface: 1) Intersecting spheres [MPS\*03] (Euclidean), 2) Growing disks, and 3) Exponential maps [SGW06] (Geodesic). Empirically, they all produce qualitatively similar results. For this paper, we use 1) with  $r = 0.0375B/R$ , where  $B$  is the diagonal of the bounding box of the surface and  $R = 5$ . In general, for surfaces with small, thin structures or substantial noise we recommend using the intersecting spheres approach. For surfaces without these features we recommend the Exponential map approach because it is faster and does not require a second parameterization step. We resample metric data evenly along the rings, at a spacing of  $2\pi r/20$ .

#### 3.1. Specific descriptors

Note: An implementation of these descriptors is available at <https://sourceforge.net/projects/meshprocessing/>.

##### Ring-based descriptors:

**[DP] Distance to plane:** Fit a plane to the ring then calculate the signed distance of each point to the plane.

**[ND] Normal distribution (2 values):** 1 - Fit a plane to the vertex, a point on the ring, and the vertex's normal. Project the ring point's normal onto that plane, and find the angle with the normal. 2 - Fit a plane to two consecutive points on the ring and the first point's normal. Project the second point's normal onto this plane. This sampling is rotation-independent.

**Curvatures:** We use four curvature values, Mean, Gaussian, Shape and Curvature index (SI, CI) [KvD92]. SI and CI map curvature values to a reasonable range using arctan and log. We apply an ad-hoc curvature normalization step to the curvatures (see Section 3.2) because otherwise large values swamp the other ones.

**[SDF] Shape Diameter function:** [SSCO08, GSCO07].

For the above descriptors we experiment with eight different approaches to sampling the data on the rings:

**[VERT]**  $R = 1, S = 1$ . Store just the data at the vertex.

**[SAL]**  $S = 1$ . Saliency sampling [LVJ05]. We used the radii as the center sampling size.

**[MIN/MAX/AVG]**  $S = 1$ . Minimum/Maximum/Average of the values on the ring.

**[MMA]**  $S = 3$ . Minimum, maximum, and averaged values.

**[DIST]**  $S = 5$ . Sort the values. Take the values that lie at the 0%, 10%, 50%, 90%, and 100% places in the sorted list.

**[HIST]**  $S = 7$ . Values at 0%, 10%, 30%, 50%, 70%, 90%, and 100%.

**[AS]**  $S = 2$ . Take the average and the standard deviation of the values on the ring.

#### Expanding descriptors:

**[LEN:]** Length of the ring over the radius.

**[AREA:]** Area of the volume in the sphere.

**[ANCE:]** Uses the ANCE [GI04] method to calculate the Mean and Gaussian curvature, using the vertex location and the re-sampled points of the ring as input.

**[FIT:]** Fit a degree two polynomial to all of the surface points inside the ring, plus the resampled ring points, weighted by distance. Calculate the Mean and Gaussian curvature from the polynomial. We use Desbrun's' [DMA02] approach to parameterize the surface.

#### Iterative operator descriptors:

**[MOV]** Movement. The distance of the vertex from its original position after applying Laplacian smoothing [DMSB99] three times for each ring.

**[HEAT]** Heat diffusion [SOG09].

Taking into account the different ways of sampling the rings, we have  $8 + 2 \times 5 + 5 \times 9 + 1 = 67$  descriptors (we throw in a descriptor which is all of the curvature metrics plus SDF sampled at the vertex).

### 3.2. Coordinate systems, normalization, and reduction

Naively comparing the resulting  $d$  vectors using an  $L^n$  norm has problems. First, the distribution of values may not be linear, or even purely exponential (see Figure 1c,d). This means that a delta difference of, eg, 0.5 may mean nearly identical for vectors with values at the extremes, but not at all the same for vectors with values at the center. Scaling by the length of  $d$  can help some, but does not really address the problem.

After computing the raw values we perform a coordinate system transformation by applying Principal Components Analysis (PCA) or Multi-dimensional Scaling (MDS) as appropriate to all descriptor values. This has an added advantage that the first eigenvector carries the bulk of the information (see Figure 1, bottom right). In this new coordinate system we apply an ad-hoc normalization to map the values in each dimension to the range  $[0, 1]$ . For the comparison studies we keep all of the dimensions. In practice, we have empirically determined that we can drop the remaining coefficients when the Eigenvalues drop below 10% of the first one without much loss. This happens around the 3rd - 10th coordinate, depending on the original dimensionality of the data (MMS - 5, DIST - 7, HIST - 10, all others 3).

We use PCA for all but the Average and Standard Deviation sample method. For this one, the correct comparison method is the *Kullback-Leibler Divergence (KLD)*. We compute a distance matrix using KLD, then apply multi-dimensional scaling (MDS) to that matrix. Because the KLD is expensive to compute, in practice we apply MDS to a  $5R \times 5R$  matrix. We select the  $5R$  vectors by adding in the vector that is furthest from any of the vectors currently selected.

**Directionality:** The eigenvectors can point in one of two ways. For visualization purposes, it is nice if the positive direction of the first eigenvector corresponds to positively curved regions, as best as possible. We determine if the first eigenvector should be flipped by comparing the coordinate directionality to either the Gaussian (Gaussian-based metrics) or the Mean (all other) curvature direction.

**Normalization:** This is a purely ad-hoc solution to the comparison. Our only justification is that the descriptor values "look" evenly distributed after the mapping (see Figure 1). Sort the coordinate values. Divide the sorted values into 5 bins, at percentages (0.0, 0.1, 0.3, 0.7, 0.9, 1.0). Within each bin, map the values to the range of the bin, optionally applying Eq. 1) one to three times. We determine how many times by choosing the mapping that is closest to a line (ie, minimizes the sum  $|x - y|$ ).

$$y(x) = e^{x^2} \text{ or } y(x) = 1 - e^{(1-x)^2} \quad (1)$$

Mean curvature: bin boundaries at 0 (-500), 0.05 (-20), 0.35 (-8), 0.5 (0), 0.65 (10), 0.95 (60) and 1 (700), with 2, 1, 0, 0, 2 applications of Eq. 1. Gaussian curvature: 0 (-40,000), 0.05 (-2000), 0.15 (-500), 0.5 (0), 0.85 (400), 0.95 (3000)

and 1 (40,000) with 2, 1, 0, 0, 2, 3 applications of Eq. 1. For both, the positive bins are reversed. These values were found by experimentation on the curvature values produced by the data sets.

#### 4. Stability study

For this study we evaluate the effects of mesh resolution, noise, and smoothing on the descriptors. We started with three meshes (fandisk, Isidore rocking horse, horse), from which we generated a total of 28 meshes with different resolutions and noise or smoothing.

**Reduction:** For each mesh we generated three meshes at different resolutions by applying QSlim [GH97] with a 30%, 60%, and 80% reduction in the percentage of faces. Even the 80% reduction did not result in a noticeable visual change. To establish the correspondence, we project the original mesh vertices onto the reduced meshes, interpolating the values in the faces. We then averaged the difference between the original and reduced descriptors across all vertices. We plot the increase in error as the mesh is reduced. For the summary plot, we used the 80% reduction values.

**Noise:** We generated clamped Gaussian noise  $\delta = e^{[-2,2]/2}$  and shifted each point along its normal  $\hat{n}$ . Let  $B$  be the diagonal of the bounding box containing the surface. We created three meshes with three noise levels,  $\pm\delta B$  (0.001, 0.0005, 0.00025) for each of the four mesh reduction levels. To generate the noise plots, we compared the noisy mesh to the unaltered mesh of the same resolution, producing four plots per descriptor.

**Smoothing:** We applied area-normalized Laplacian smoothing [DMSB99]. At each iteration we moved each point  $1/3$  of the way to its Laplacian average, then area-normalized. We generate meshes and plots as for the Noise case.

Figure 2 summarizes the results across all descriptors and all studies, and shows example individual plots for the mesh reduction and noise and smoothness. Complete plots are available in the supplementary materials. For all measures, we used the  $L^2$  norm.

We saw the same general trends in all three studies, in terms of the behavior of the descriptors. Distance to plane and Normal distribution were the most stable descriptors, with Mean, CI, SI, and Gauss roughly similar. SDF was the next most stable, followed by Movement and Point (combining Mean, Gauss, SI, CI, SDF, and Movement at the point). Length of Curve, followed by the four fitting descriptors (ANCE and FIT), were not that stable.

For the sampled descriptors, the best sampling strategy was the histogram one (seven samples) followed closely by the distribution descriptor (five samples) then MMA (three samples). AVG, Saliency, and MIN/MAX were, on average, the same, with AVG slightly out-performing the others. Average and Standard deviation (AS) and Vertex were not very stable, with Vertex being very unstable.

We analyzed the effects of mesh resolution, noise, and sampling independently by looking at the individual plots. In summary, we saw the following: 1) Adding noise affects the higher resolution meshes more than it does the lower resolution ones. 2) Smoothing tends to affect the lower resolution meshes more than the higher resolution ones. 3) The smoother or “nicer” the mesh is to start with the less adding noise or smoothing makes a difference. 4) Using multiple rings produced an order of magnitude improvement over simply using the descriptor calculated at the vertex. 7) Additional averaging (saliency sampling, fitting) was, surprisingly, more prone to error than sampling using rings. 8) SI and CI are slightly more stable than our (normalized) Mean and Gauss curvature, with Gauss being the most unstable.

#### 5. Sensitivity study

The previous study looked at the stability of the descriptors — how much they were influenced by noise, mesh sampling, and smoothing. In these studies, we evaluate the descriptors by how well they can distinguish features. For each data set (mandible (10), ferret (8), bat ears (35), mechanical parts (4)) we hand-picked sets of points which should be similar (the “same” point on different instances of similar meshes). Each set was chosen to be sufficiently different from the other ones. This is, admittedly, a human-perception biased method of creating an evaluation set. However, given that we want to work with real data sets, not artificially generated ones, we believe it is justified.

**Data analysis:** Ideally, points in one set should have descriptors that are similar, while points in other sets should have descriptors that are dissimilar. We picked two measures to evaluate this. The first measure is simply the spread of a given shape descriptor’s feature value over all the points in the set. These values are summed up over all of the sets to yield a score for each shape descriptor. A zero average and narrow standard deviation are good.

The second measure evaluates how distinctive the shape descriptors are, i.e., how likely a point from one set is to match to points in another set. To calculate this, we compare each point to all of the other points, and sort the results. We then count how far down the list we have to go to find a point in the same set. Ideally, the count should be zero.

We summarize the results in Figure 3. We combine both scores into a single plot by plotting the first measure, and the second measure normalized to the first measure. The mean and normal descriptors are clearly the best, followed by distance to the plane and Gauss. Not too surprising, sampling each ring with 3-7 samples (MMS, DIST, HIST) performed better than taking a single sample on the ring. For the mechanical models alone, MMS was the better choice (see supplemental).

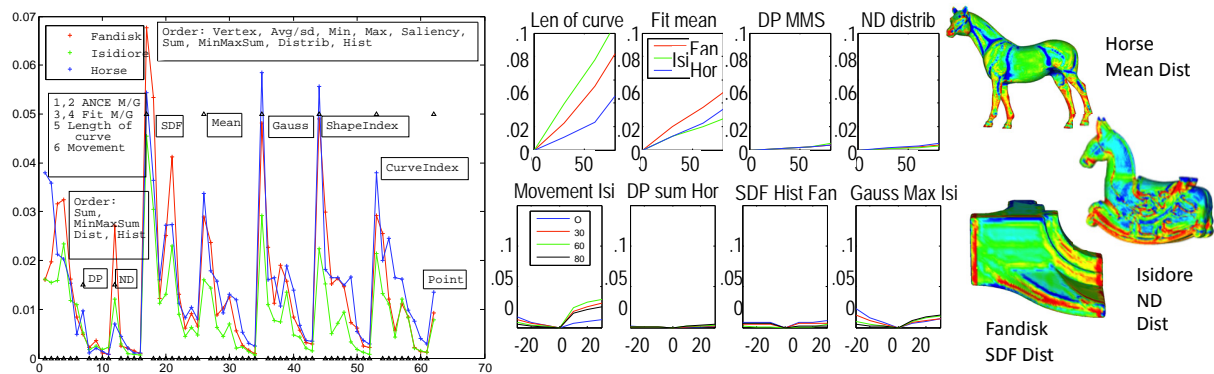


**Figure 2:** Left: All of the descriptors. For each data set we averaged across all 28 meshes. The total score for a descriptor was a blended combination of the average and the max (3/4 and 1/4, respectively). The descriptor values range from zero to one, so a y axis value of 0.01 means the average difference is less than 1% of the maximum descriptor value. Middle: Top: Mesh reduction. x-axis is the mesh reduction amount, y-axis is the difference in the descriptors, averaged across the surface ( $\|$  reduced - original  $\|$ ). Bottom: Noise and smoothness. x-axis goes from noisy to smooth. The meshes were compared to their original mesh of the same resolution.

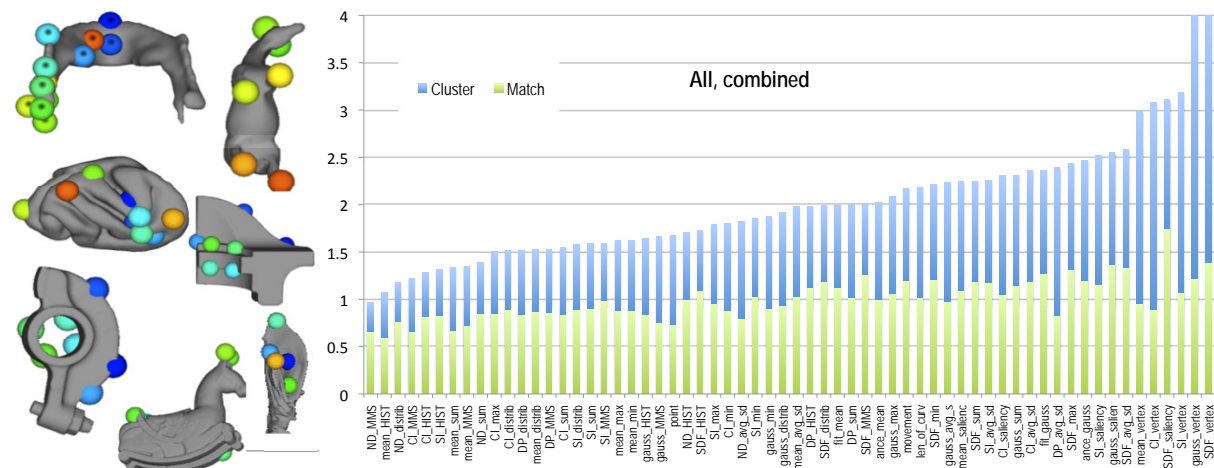


**Figure 3:** Local feature selectivity. a) Examples of selected points. Note: Ball size is the actual size of the largest ring. b) Yellow bars: Average spread of the shape descriptor values from the mean. A smaller spread is better. Blue bars: How likely a point was to match to another point in the same set. Zero is better. Both measures were divided by their mean in order to combine them in one plot.

## 6. Correlation study

An obvious question to ask is, if one descriptor is good, would two be better? We did not explicitly compare combining descriptors, but we did perform a correlation study (see Figure 4). The strongest correlations are, of course, between different samplings of the same descriptor. SDF correlates the most strongly with itself, followed by Mean curvature, Normal Distribution, and Distance to Plane. Gaussian curvature did not show much correlation. Of the remaining descriptors, Movement and Length of Curve did not correlate strongly with much else. Of the two, Movement is better for both noise and sensitivity, making it a good candidate

to combine with either the Normal Distribution or the Mean curvature.)

## 7. Results and discussion

The studies clearly show that sampling data just at a vertex is bad; this is not surprising. The general trend, for all of the descriptors, is that more samples is better, both for stability and discrimination, regardless of the descriptor used. We did see evidence of over-fitting for the highest level of sam-

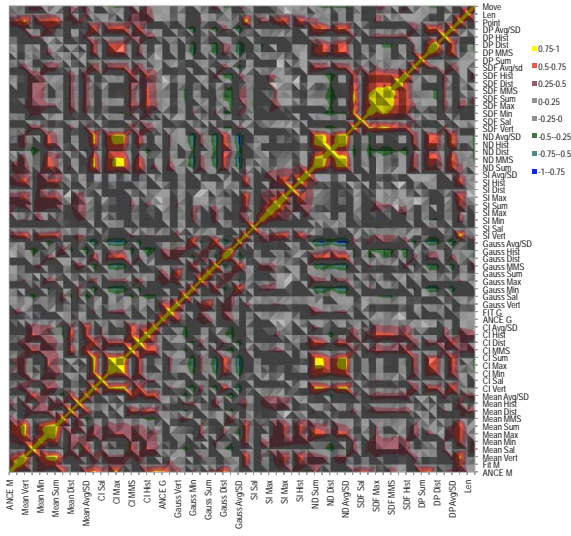


Figure 4: Correlations of descriptors over all data sets.

pling in the sensitivity tests, which indicates that the ideal sampling is somewhere around 3-5 samples per ring, which can be reduced to 7-10 samples total via PCA. The Normal distribution descriptor is consistently the best, followed by Mean curvature or the Curvature index.

The non-sampled descriptors (Movement, Length of curve) did about as well as the one sample per ring version of the other descriptors, which indicates that it is primarily the increased sampling that is of benefit. Not too surprisingly, the Shape Diameter Function is less discriminating locally than other descriptors since, in a sense, it is measuring mid-scale features in the form of the local medial axis.

One surprising result is that the ranking for stability is similar for the ranking for discrimination power. This hints that the ability to filter out small geometry changes is related to the ability to cluster similar local shapes.

Limitations of the study: Obviously, there are many ways that local shape descriptors can be constructed, and there may be unintended biases in the particular implementations we use (for example our ad-hoc normalization). We also only evaluated the feature matching task at small scales; for segmentation a different descriptor may be more appropriate.

**Timings:** For smaller meshes (< 30,000 vertices) the descriptors are roughly equivalent, at 2-10 seconds per descriptor (Movement being much faster, ANCE and Fit being slowest). For bigger meshes, finding the rings dominates the calculations (up to an hour for 70,000 vertices). Area and SDF also do not scale well. Saliency and avg/sd are the slowest ring sampling methods, with the others about equal. The PCA and normalization calculations are dominated by the length of the vector; a few seconds for most of the descrip-

tors, up to a couple of minutes for the histogram sampling on large (> 70,000) meshes.

**Acknowledgements:** Funded in part by NSF grants CCF 0702662 and DBI 1053171.

## 8. Conclusion

We have presented a systematic evaluation of local shape descriptors for the task of local feature matching on real data sets, both biological and man-made. This was accomplished by creating a unifying framework for the disparate local shape descriptors.

## References

- [BBK\*10] BRONSTEIN A. M., BRONSTEIN M. M., KIMMEL R., MAHMOUDI M., SAPIRO G.: A gromov-hausdorff framework with diffusion geometry for topologically-robust non-rigid shape matching. *Int. J. Comput. Vision* 89 (September 2010), 266–286. 3
- [BMP02] BELONGIE S., MALIK J., PUZICHA J.: Shape matching and object recognition using shape contexts. *IEEE Trans. Pattern Anal. Mach. Intell.* 24, 4 (2002), 509–522. 2
- [CGR\*04] CLARENZ U., GRIEBEL M., RUMPF M., SCHWEITZER M. A., TELEA A.: Feature sensitive multi-scale editing on surfaces. *Vis. Comp.* 20 (Jul 2004), 329–343. 2
- [CJ97] CHUA C. S., JARVIS R.: Point signatures: A new representation for 3d object recognition. *Int. J. Comput. Vision* 25, 1 (1997), 63–85. 1, 2, 3
- [Con86] CONNOLLY M. L.: Measurement of protein surface shape by solid angles. *J. Mol. Graph.* 4 (March 1986), 3–6. 2
- [CPJG09] CIPRIANO G., PHILLIPS JR. G. N., GLEICHER M.: Multi-scale surface descriptors. *IEEE Trans. on Viz. and CG* 15 (November 2009), 1201–1208. 2
- [CRT04] CLARENZ U., RUMPF M., TELEA A.: Robust feature detection and local classification for surfaces based on moment analysis. *IEEE Trans. on Viz. and CG* 10 (September 2004), 516–524. 2
- [dGGV08] DE GOES F., GOLDENSTEIN S., VELHO L.: A hierarchical segmentation of articulated bodies. In *SGP '08* (2008), SGP '08, pp. 1349–1356. 3
- [DMA02] DESBRUN M., MEYER M., ALLIEZ P.: Intrinsic parameterizations of surface meshes. *Computer Graphics Forum* 21 (2002), 209–218. 4
- [DMSB99] DESBRUN M., MEYER M., SCHROEDER P., BARR A. H.: Implicit fairing of irregular meshes using diffusion and curvature flow. In *SIGGRAPH '99* (1999), pp. 317–324. 4, 5
- [FSD99] FISCHL B., SERENO M. I., DALE A. M.: Cortical surface-based analysis: Inflation, flattening, and a surface-based coordinate system. *NeuroImage* 9, 2 (1999), 195 – 207. 3
- [GGZ05] GATZKE T., GRIMM C., GARLAND M., ZELINKA S.: Curvature maps for local shape comparison. In *Shape Modeling and Applications* (2005), pp. 246–255. 2
- [GH97] GARLAND M., HECKBERT P. S.: Surface simplification using quadric error metrics. In *SIGGRAPH '97* (1997), pp. 209–216. 5
- [GI04] GOLDFEATHER J., INTERRANTE V.: A novel cubic-order algorithm for approximating principal direction vectors. *ACM Trans. Graph.* 23, 1 (2004), 45–63. 4

- [GSCO07] GAL R., SHAMIR A., COHEN-OR D.: Pose-oblivious shape signature. *IEEE Trans. on Viz. and CG* 13 (March 2007), 261–271. 3, 4
- [KPNK03] KORTGEN M., PARK G. J., NOVOTNI M., KLEIN R.: 3d shape matching with 3d shape contexts. In *the 7th Central European Seminar on Computer Graphics* (April 2003). 2
- [KvD92] KOENDERINK J. J., VAN DOORN A. J.: Surface shape and curvature scales. *Image Vision Comput.* 10 (October 1992), 557–565. 4
- [LG05] LI X., GUSKOV I.: Multi-scale features for approximate alignment of point-based surfaces. In *SGP 2005* (2005). 3
- [LVJ05] LEE C. H., VARSHNEY A., JACOBS D. W.: Mesh saliency. *ACM Trans. Graph.* 24 (July 2005), 659–666. 2, 4
- [MPS\*03] MORTARA M., PATANE G., SPAGNUOLO M., FALCIDIENO B., ROSSIGNAC J.: Blowing bubbles for multi-scale analysis and decomposition of triangle meshes. *Algorithmica* 38, 1 (2003), 227–248. 2, 3
- [OS10] ONG J. L., SEGHOUANE A.-K.: From point to local neighbourhood: Polyp detection in ct colonography using geodesic ring neighbourhoods. *IEEE Trans Image Process* (2010). 2
- [PWHY09] POTTMANN H., WALLNER J., HUANG Q.-X., YANG Y.-L.: Integral invariants for robust geometry processing. *Comput. Aided Geom. Des.* 26 (January 2009), 37–60. 2
- [Rus07] RUSTAMOV R. M.: Laplace-beltrami eigenfunctions for deformation invariant shape representation. In *SGP 2007* (2007), pp. 225–233. 3
- [SGW06] SCHMIDT R., GRIMM C., WYVILL B.: Interactive decal compositing with discrete exponential maps. In *SIGGRAPH '06* (2006), ACM, pp. 605–613. 3
- [SM92] STEIN F., MEDIONI G.: Structural indexing: Efficient 3-d object recognition. *IEEE Trans. Pattern Anal. Mach. Intell.* 14, 2 (1992), 125–145. 2
- [SOG09] SUN J., OVSJANIKOV M., GUIBAS L.: A concise and provably informative multi-scale signature based on heat diffusion. In *SGP '09* (2009), SGP '09, pp. 1383–1392. 3, 4
- [SSCO08] SHAPIRA L., SHAMIR A., COHEN-OR D.: Consistent mesh partitioning and skeletonisation using the shape diameter function. *Vis. Comput.* 24 (March 2008), 249–259. 4
- [YF99] YAMANY S. M., FARAG A. A.: Free-form surface registration using surface signatures. In *ICCV '99* (1999), IEEE Computer Society, p. 1098. 2
- [YF02] YAMANY S. M., FARAG A. A.: Surfacing signatures: An orientation independent free-form surface representation scheme for the purpose of objects registration and matching. *IEEE Trans. Pattern Anal. Mach. Intell.* 24, 8 (2002), 1105–1120. 2, 3
- [ZG04] ZELINKA S., GARLAND M.: Similarity-based surface modelling using geodesic fans. In *SGP '04* (2004), ACM, pp. 204–213. 3